Random Dynamics from Time Series of Rotating Fluid

Yuzuru Sato,[1,*] Makoto Iima,[1] and Yuji Tasaka[2]

[1] *RIES / Department of Mathematics, Hokkaido University, Kita 12 Nishi 6, Kita-ku, Sapporo 060-0812, Japan*

[2] *Graduate School of Engineering, Hokkaido University, Kita 13 Nishi 8, Sapporo, 060-8628, Japan.*

A random dynamics is extracted from time series of laminar-turbulent transition in rotating fluid in an open cylinder. We focus on the dynamics of the surface height in the central region and measure switching dynamics between different quasi-stationary states and intensity of underlying turbulence. Density of return map is constructed from an one dimensional map with an stochastic term from the experimental data. It is shown that the random dynamics whose noise amplitude depends on the slow variable describes the observed macroscopic features of rotating fluid in terms of noise-induced phenomena.

PACS numbers: 47.32.Ef, 05.45.-a, 89.75.Fb
Keywords: Surface switching, Multiscale dynamics, Random dynamical systems, Noise-induced phenomena

Multiscale phenomena in dynamical systems with large degree of freedom is an important problem in nonlinear physics. In number of studies, abstract dynamical systems models have been used to analyze hierarchical state space structure. A typical multiscale phenomena which has been analyzed with dynamical systems theory is laminar-turbulent transition [1]. Recently, in the turbulence of pipe flow, transient dynamics has been investigated discussing the lifetime of transitory behavior in the limit of the large Reynolds number [2]. In these models, the set of initial conditions separating eventual state, either laminar or turbulent, forms a chaotic attractor except one dimensional unstable manifold. The finite lifetime implies that the set of turbulent state is not closed, and any states in the turbulent state come back to the laminar state within finite time. The pipe flow has a simple geometry, which enables us to obtain mathematically clean models. However, many other laminar-turbulent transition including free surface flow, which we treat in this paper, does not have such advantage. Several theoretical models based on the separation between fast motion and slow motion has been also proposed; models by the extraction of slow motion, models using appropriate coarse-graining of phase space, or fully phenomenological models by using stochastic dynamics [3, 4].

Here, we focus a macroscopic motion of the surface shape of fluid, which is called "surface switching", in an open cylinder driven by constant rotation of the bottom [5]. Around the critical Reynolds number for the laminar-turbulent transition, the surface deformation shows irregular switching between axisymmetric shapes and non-axisymmetric ones even when the rotation speed is constant. While the time scale of the switching phenomena is considerably slow compared to the rotation speed, the motion of the surface height in the central region is strongly correlated with the underlying turbulence intensity. In other words, the surface shape plays a role of high-dimensional control parameter of the flow states, and the flow state determines the surface shape, in turn. The turbulent flow generates large fluctuation affecting the macroscopic dynamics of the surface height.

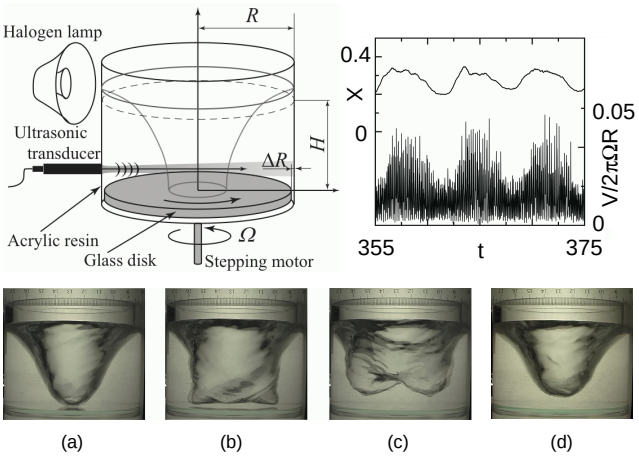

FIG. 1: (Top-Left) Experimental set-up for the measurements slow and fast motion of the flow and the experimental time series of the surface height and rotating flow. (Top-Right) In time series, horizontal axis denotes time [sec] and vertical axis is for the ratio of the surface height x and the ratio of the turbulence intensity $V/2\pi\Omega R$, which are both normalized in $[0, 1]$ with respect to the maximum. (Bottom) The global surface shape of (a) axisymmetric state, (b) non-axisymmetric deformation, and (c) double-well shape detached from the bottom. (d) axisymmetric state elongated to the bottom.

In this paper, we reduce experimental data into simple random dynamical systems model. It is shown that one dimensional map with noise whose amplitude depends on the slow variable describes the observed macroscopic features of the surface switching phenomena. The return map and embedding methodology [6] is extended with an appropriately designed stochastic term to describe macroscopic slow motion in deterministic dynamical systems with a large degrees of freedom. We succeed in reproducing the switching phenomena between multiple quasi-stationary states, which has a globally disordered

flow patten, and qualitative bifurcation structure including hysteresis. It is also shown that the noise amplitude depending on the state is crucial, suggesting that studies on noise-induced phenomena can be a good theoretical approaches to this multiscale phenomena.

A schematic outline of the experimental set-up to observe the surface switching is shown in FIG. 1, Top-Left [7]. The open ended cylindrical vessel is made of acrylic resin; the inner radius is $R = 42$ mm. A glass disk mounted at the bottom of the vessel is connected to a stepping motor through a shaft. There is a gap of $\Delta R = 0.3$ mm between the disk and the sidewall of the vessel, which works as a trigger noise source. The vessel was filled with tap water; the liquid height at rest was $H = 40$ mm. Particles of porous resin were mixed into the water as tracers for the velocity profile measurements. The rotating speed of the disk Ω was varied from 300 to 850 rpm. In this range, the Reynolds number $Re = 2\pi\Omega R/\nu$, where ν is the kinematic viscosity of water, varies from 0.55×10^5 to 1.57×10^5. An ultrasonic transducer is mounted at the disk to measure the moving average of the height of the center of the surface h giving a normalized slow variable $x = h/H$, and to measure the normalized turbulence intensity $V/2\pi\Omega R$, where V is the spatial average of the root mean square of the flow velocity $u_{rms}(r)$ distributed over the radius r. In this way, we measure time series with two largely different time scales at the same time (FIG. 1, Top-Right).

A typical surface switching proceeds as follows (FIG. 1, Bottom): (i) the bottom of the axisymmetric surface elongates and attaches to the rotating disk; (ii) the axisymmetry of the free surface breaks down and the transition to a double-well shape occurs; (iii) the horizontal deformation of the free surface becomes larger and finally the surface is fully detached from the bottom; (iv) the bottom of the surface moves to a higher position and the surface rotates uniformly with a double-well shape with two distinct humps; (v) the free surface reverts to an axisymmetric shape and is elongated to the bottom.

We set Reynolds number close to the critical value for the laminar-turbulent transition, and measure two physical quantities; surface height in the central region, and intensity of turbulence outside the central region. Around this region, roughly, when the surface height is large and the surface shape is non-axisymmetric, the flow is turbulent with large energy dissipation. When the height is small and the shape is axisymmetric, the flow is laminar with small energy dissipation. The heterogeneity of energy dissipation rate depending on the surface height makes the switching motion a robustly observed phenomenon.

The return plot of the maximum and the minimum of the moving averaged time series of the surface height (FIG. 2, Top-Left) has an uni-modal structure with partial one dimensionality (FIG. 2, Top-Right), indicating that the slow motion involves stochastic causality. There

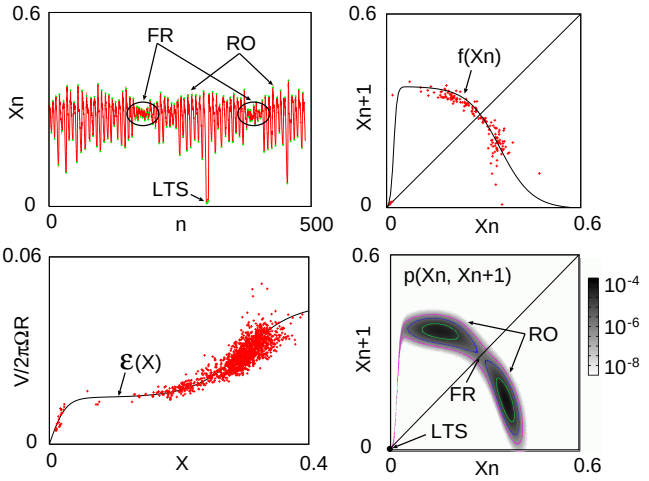

FIG. 2: (Top-Left) The experimental time series of the surface height. Three quasi-stable states, RO, FR, and LTS are indicated in the time series. (Top-Right) the return plot and the model for deterministic term based on Eq. (2) with $A = 0.38$, $\beta_1 = 200$, $\beta_2 = -20$, $p = 0.0215$, $q = 0.39$. (Bottom, left) Intensity of turbulence and the model for stochastic term based on Eq. (3) with $B = 0.04$, $\beta_3 = 15$, $\beta_4 = 50$, $r = 0.4$, and $\delta = 10^{-8}$. (Bottom-Right) Return map density $p(x_n, x_{n+1})$ generated by the model (1). It is a normalized histogram of numerical simulation data with 10^8 iterations of the random map for the orbit x_n with random initial conditions, multiplied by 10^6 different independent noise realization of ξ_n. The density at the origin $p(0,0) \sim 10^{-4.75}$ is denoted with a black point.

are three experimentally observed quasi-stationary states in the rotating fluid; regular oscillation (RO), flat rotation (FR), and laminar-turbulent switching (LTS) [7], which is depicted in the time series. Taking the average over each x the deterministic return map is given as a function $f(x)$. The experimental data of the intensity of turbulence is given in FIG. 2, Bottom-Left. The average of the turbulence intensity is given as a function $\epsilon(x)$. Unlike the standard return map methodology, our interpretation of the results is that one dimensional deterministic dynamics is observed for small x close to 0 and higher dimensional or stochastic dynamics is observed for larger x.

We introduce a simple random dynamical system model to describe the motion of surface height;

$$x_{n+1} = f(x_n) + \xi_n(x_n) \tag{1}$$

For the deterministic term, we give the following model approximately obtained from the return plot of the slow surface motion (Fig. 2, Top-Right);

$$f(x) = \begin{cases} A\left[\frac{1}{1+e^{-\beta_1(x-p)}} - \frac{1}{1+e^{\beta_1 p}} + \frac{1}{1+e^{-\beta_2(x-q)}} - \frac{1}{1+e^{\beta_2 q}}\right] & (x \geq 0) \\ 0 & (x < 0) \end{cases} \tag{2}$$

The stochastic term $\xi_n(x_n)$ is modeled by a random variable obeying white Gaussian distribution, whose amplitude is a function of the surface height, $\xi_n(x) = \epsilon(x)\xi_n$, where

$$\epsilon(x) = B\left[\frac{e^{\beta_3 r} - e^{-\beta_3(x-r)}}{(1+e^{-\beta_3(x-r)})(1+e^{\beta_3 r})} + \frac{1-e^{-\beta_4 x}}{2(1+e^{-\beta_4 x})} + \delta\right] \tag{3}$$

and $\xi_n \sim N(0,1)$, which is also approximately obtained from the integrated fast motion (FIG. 2, Bottom-Left).

By using the model (1), we numerically generate "return map density" $p(x_n, x_{n+1})$, which is the orbit density at the point (x_n, x_{n+1}) (FIG. 2, Bottom-Right), and is interpreted as the natural invariant density for possible return maps. Note that the return map density is not a simple combination of deterministic and stochastic term in the model (1). It is a density deformation induced by interaction between deterministic dynamics and stochastic noise. Generated density represents stochastic causality of slow motion embedded in high-dimensional dynamics. High density region indicates each of three quasi-stationary states, RO, FR, and LTS.

We study bifurcation of the model (1) numerically. We are interested in the system behavior near the critical parameters given as in FIG. 2. For increasing the nonlinearity of the map A causes instability, we assume that A corresponds to the Reynolds number. In FIG 3, Top-Left illustrates the phase diagram for the parameters A and B. There are five phase; (i) Irregular motion due to strong noise, (ii) Attractor selection (irregular selection of two attractors due to large noise), (iii) Bistabe, (iv) Surface switching, and (v) Local switching (switching between RO and FR with small noise.). The deterministic bifurcation varying the parameter A with $B = 0$ fixed, is shown in FIG 3, Middle-Left. In the bifurcation diagram, $A_1 = 0.3715$ is a deterministic period-doubling bifurcation point. The bistability ends at the point $A_3 = 0.3798$ with disappearance of the fixed point $x = 0$. The surface switching begins at $A_2 = 0.372$; The small noise effectively destabilizes the stable fixed point $x = 0$ before the deterministic saddle-node bifurcation point A_3. The model (1) with the parameters in FIG. 2 reproduces the observed macroscopic feature qualitatively in a broad region of the phase diagram (FIG 3, Top-Left).

The deterministic term described by $f(x)$ can potentially show both type I and III intermittency. When $A = 0.38$ and $B \sim 0$, we have two unstable fixed points; a nearly tangential fixed point M_0 at $x = 0$, whose derivation of the map is close to 1, and a weakly repelling fixed point M_1 at $x \sim 0.311$ whose derivation of the map is close to -1. A period two limit cycle M_2 surrounding the unstable fixed point M_1 is globally asymptotically stable. Based on these state space structures, M_0, M_1, and M_2, depicted in FIG. 3, Bottom,the three quasi-stationary states, LTS, FR, and RO emerges by noise. With the stochastic term $B > 0$, the radius of period two cycle

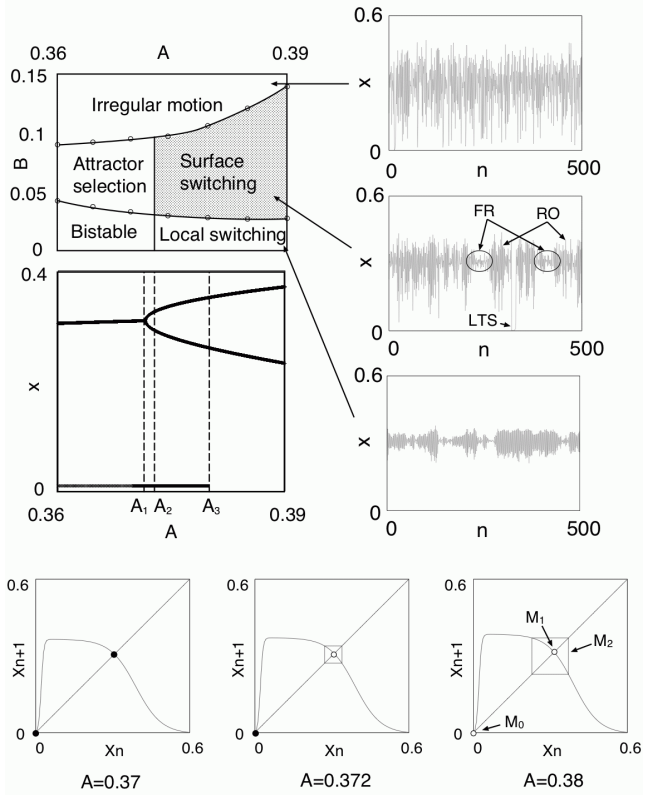

FIG. 3: (Top-Left) Phase diagram of the dynamics in the model (1) for $A \in [0.36, 0.39]$ and $B \in [0.0, 0.15]$ with the other parameter set to the same as those in FIG. 2. (Middle-Left) The bifurcation of the deterministic limit, $x_{n+1} = f(x_n)$ with $B = 0$, is also shown below for a reference. $A_1 = 0.3715$ is a deterministic bifurcation point. $A_2 = 0.372$ is the point where the surface switching begins. Deterministic bistability ends at the point $A_3 = 0.3798$. (Top-Right) With $A = 0.38$ and varying B, local switching ($B = 0.01$), global surface switching ($B = 0.04$), and irregular motion ($B = 0.1$), are observed in each region, respectively. (Bottom) Fixed points and limit cycle in the deterministic limit are shown for $A = 0.37$, $A = A_2 = 0.372$, and $A = 0.38$. Black and white circles denotes stable and unstable fixed points.

may fluctuate to switch M_1 and M_2, corresponding FR and RO. The weakly repelling properties of the unstable fixed point M_1 supports emerging stagnant motion near M_1 as a noise-induced phenomenon. When the fluctuation becomes large, x can be larger and then go back near $x = 0$. Close to M_0, the orbits are trapped by the almost deterministic tangency, resulting LTS. After escaping the narrow channel, the local switching between RO and FR recovers. As a result, we observe three quasi-stationary states of slow motion and switching between them.

Phenomenological interpretation is the following. The deterministic term $f(x)$ describes energy injection and A plays the role of energy injection rate. The stochastic term $\xi_n(x)$ describes energy dissipation and B plays the role of energy dissipation rate. Starting with local

switching between RO and FR with underlying turbulent flow, the total energy dissipation is growing and, eventually, the flow becomes laminar and the surface is deformed to the axisymmetric shape going down to the bottom. At the bottom, with the constant energy injection and the small dissipation, the total energy amount is growing. Finally, the surface is deformed to the non-axisymmetric shape and the flow becomes turbulent, resulting LTS. Thus, balancing energy injection and dissipation, the switching phenomenon between three quasi-stationary states, RO, FR, and LTS are robustly observed.

We adopt equation (3) to reproduce experimentally observed hysteresis of the time average of turbulence intensity $\overline{V/2\pi\Omega R}$ based on the underlying bifurcation along A in the model (1). Without stochastic term, the model (1) shows bistability and the period-doubling bifurcation for larger A. With $B = 0.04$, the hysteresis in the time average of the noise amplitude $\overline{\epsilon(x)}$ occurs from $A = A_0 \sim 0.10$ to $A = A_2 \sim 0.372$, when we slowly varies A from small value to large value and vise versa (FIG. 4). These hysteresis mainly depends on the structure of the deterministic return map. We note that, in our model, the unbounded noise in the stochastic term makes dynamics eventually converge to one of the quasi-stationary state in theoretical limit. On the other hand, three quasi-stationary states are not strongly attracting and dynamics is almost always transitory. Thus, in numerical simulation of our model, the parameter range of occurrence of the hysteresis changes by trials with a large variance, implying that it is a phenomenon observed on finite time scales. However, we expect that a similar mechanism exists also in the experiments, which is based on a single long-run measurement and slowly varying Reynolds number, again, on finite time scales. If the relative noise effect is much larger than the present setting, this hysteretic phenomenon should disappear. A new experiment controlling the trigger noise (e.g. those with different ΔR) seems to be successful for controlling the width of the hysteresis region, which is expected from the presented theory.

We presented a random dynamical system model of surface switching in rotating fluid, which is directly extracted from experimental time series. The return map density describes the stochastic causality in the slow motion in the deterministic high-dimensional dynamics. Macroscopic features of the phenomena, irregular switching and hysteresis of turbulence intensity are reproduced by the model and the resulting numerical simulation are interpreted as a noise-induced phenomenon. For further development of this framework, we refer to studies on more complex noise induced phenomena in generic nonlinear dynamics with presence of strong perturbation, which has been extensively investigated recently [8]. This paper established possible theoretical connections between presented random dynamics modeling for multi-

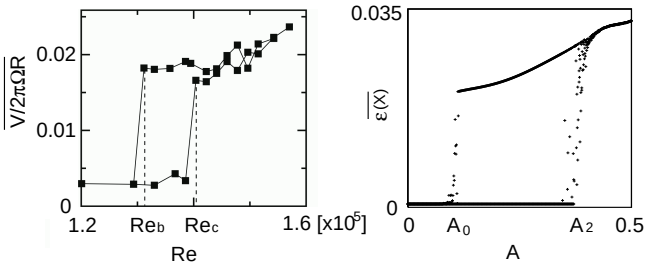

FIG. 4: (Left) Hysteresis of time average of turbulence intensity $\overline{V/2\pi\Omega R}$ in the experiment. (Right) Hysteresis of time average of the noise amplitude $\overline{\epsilon(x)}$ in the model (1) with $B = 0.04$. Hysteresis with slowly varying Re and A from small value to large value and vise versa, are depicted based on a single long path for both the experiment and the model. $Re_b = 1.29 \times 10^5$ and $A_0 = 0.10$ are the point where the bistability begins, and $Re_c = 1.40 \times 10^5$ and $A_2 = 0.372$ are the point where the bistability ends and switching phenomenon begins, in the average in the experiment and in the model, respectively.

scale dynamics and studies on noise induced phenomena. The presented framework may shed a light on understanding complex multiscale dynamics, when the random dynamics model is extended to the one over several scales. The techniques for extracting random dynamics from observed time series should be directly applicable to various types of laminar-turbulent transition, as well as any other physical systems when such a stochastic causal structure exists at macroscopic levels. Studies on extracting methods of random dynamics from higher-dimensional deterministic dynamics, investigation of return map densities and its applications, and rigorous analysis of the extracted models in terms of random dynamical systems theory [9] will be done elsewhere.

* Electronic address: ysato@math.sci.hokudai.ac.jp

[1] J. P. Gollub and H. L. Swinney, Phys. Rev. Lett. **35**, 927 (1975).

[2] B. Hof, J. Westerweel, T. Schneider, and B. Eckhardt, Nature **443**, 59 (2006), J.D. Skufca, J. A. Yorke and B. Eckhardt, Phys. Rev. Lett., **96**, 174101 (2006), T. Schneider, B. Eckhardt and J. Yorke, Phys. Rev. Lett., **99**, 034502 (2007), B. Eckhardt, Nonlinearity, **21**, T1 (2008).

[3] A. Torre and J. Burguete, Phys. Rev. Lett. **99**, 054101 (2007).

[4] W. Just, K. Gelfelt, N. Baba, A. Riegert, and H. Kantz, J. Stat. Phys. **112**, 272 (2003).

[5] T. Suzuki, M. Iima, and Y. Hayase, Physics of Fluids **18**, 101701 (2006), Y. Tasaka, K. Ito and M. Iima, Journal of Visualization, **11**, 163 (2008), Y. Tasaka, M. Iima and K. Ito, J. Phys.: Conf. Ser., **137**, 012030 (2008).

[6] R. S. Shaw, *The Dripping Faucet as a Model Chaotic Sys-*

tem (Aerial Press, Santa Cruz, California, 1984), N. H. Packard and J. P. Crutchfield and J. D. Farmer and R. S. Shaw, Phys. Rev. Lett., **45**, 712 (1980).

[7] Y. Tasaka and M. Iima, J. Fluid. Mech. **636**, 475 (2009).

[8] G. Mayer-Kress and H. Haken, Journal of Statistical Physics **26**, 149 (1981), K. Matsumoto and I. Tsuda, Journal of Statistical Physics, **31**, 87 (1983), Z. Liu, Y-C. Lai, L. Billings, and I. B. Schwartz, Phys. Rev. Lett., **88**, 124 (2002), T. Tel and Y-C. Lai, Phys. Rev. E, **81**, 05620 (2010), Y. Sato and D. Albers, (2011) submitted, Y. Sato and Y. Iwata (2011) submitted.

[9] A. Lasota and M. Mackey, *Chaos, Fractals, and Noise* (Springer, 1991), K. R. Schenk-Hoppe, Discrete and Continuous Dynamical Systems, **4**, 99 (1998).